Solar-Terrestrial Physics. 2024. Vol. 10. Iss. 4. P. 19–27. DOI: 10.12737/stp-104202403. © 2024
V.I. Mordvinov, E.V. Devyatova, V.M. Tomozov. Nikolaishvili. Published by INFRA-M Academic Publishing House

DOI: 10.12737/stp-104202403

Received June 17, 2024
Accepted October 22, 2024

DEPENDENCE OF NORMAL MODES OF THE BAROTROPIC VORTEX EQUATION ON THE MEAN FLOW STRUCTURE AND NUMERICAL SIMULATION PARAMETERS

V.I. Mordvinov
Institute of Solar-Terrestrial Physics SB RAS, Irkutsk, Russia, v_mordv@iszf.irk.ru

E.V. Devyatova
Institute of Solar-Terrestrial Physics SB RAS, Irkutsk, Russia, devyatova@iszf.irk.ru

V.M. Tomozov
Institute of Solar-Terrestrial Physics SB RAS, Irkutsk, Russia, tom@iszf.irk.ru

Abstract. We present the results of numerical simulations of normal modes of the mean flow due to the superposition of cyclonic and anticyclonic vortices at high latitudes. Such a flow structure is often observed in the upper troposphere — the lower stratosphere in winter. Our aim is to identify normal modes in the oscillation spectrum that resemble torsional oscillations. We solve the problem numerically, using a barotropic quasi-geostrophic model. Additionally, we estimate the dependence of the normal modes on experimental parameters (the number of spherical harmonics in the stream function field expansion, the parameterization of viscosity and hyperviscosity).

The simulation results show that flow instability almost always increases with increasing amplitude of the anticyclonic vortex to varying degrees at different viscosities and different numbers of harmonics in the field expansion. The spatial structure of the most unstable normal modes changes most chaotically when the experiment parameters and the mean flow change. This significantly complicates the interpretation of real oscillations in terms of normal modes, including the interpretation of torsional oscillations. Axisymmetric normal modes are often present in the spectrum, but they do not have all the properties of torsional oscillations and do not dominate the spectrum.

Keywords: hydrodynamics, atmosphere, normal modes, torsional oscillations.

INTRODUCTION

Much attention in atmospheric physics is paid to the study of low-frequency oscillations with periods from several days to several tens of days, having a large-scale structure along latitudinal circles. Of particular interest were the disturbances running in the zonal direction with periods of 4, 5, 10, 16, 25 days [Kasahara, 1980; Branstator, 1987; Branstator, Held, 1995; Madden, 2007; Pogoreltsev et al., 2009; Koval et al., 2018], as well as quasi-stationary oscillations — teleconnections [Simmons et al., 1983; Blackmon et al., 1984a, b]. To interpret oscillations in the upper atmosphere, a theory of eigenoscillations of the atmosphere at rest was developed. Under this assumption, eigenoscillations of the atmosphere, called normal modes, are solutions of Laplace tidal equations [Jaglom, 1953; Longuet-Higgins, 1964, 1968; Dikii, 1969]. However, in the lower layers of the atmosphere, such an assumption is incorrect since the atmosphere is not at rest, and the mean flow is not zonally symmetric. In this case, instead of the Laplace tidal equation, we get an eigenvalue problem and eigenfunctions of the differential operator depending on the mean flow [Dymnikov, Skiba, 1986; Dymnikov, 2007; Dymnikov, Filatov, 1988]. These oscillations have also been called normal modes, which sometimes causes confusion in the interpretation of research results. In this paper, we employ the definition of normal modes from [Dymnikov, Filatov, 1988] and call them new normal modes (NNMs).

In the NNM spectrum, unstable components appear whose amplitude increases with time; therefore, the normal mode method is widely used to analyze the stability of mean flows. Theoretical and applied research in this area can be found in works by Russian and foreign authors [Simmons et al., 1983; Dymnikov, Filatov, 1988; Branstator et al., 1995; Dymnikov, 2007]. We assume that these modes can also explain torsional oscillations.

Torsional oscillations are disturbances propagating in the meridional direction, determined by low-frequency filtering and zonal averaging [Zorkaltseva et al., 2019]. These disturbances may be eigenoscillations of the atmosphere (as we have suggested) or result from nonlinear processes such as the interaction between traveling and stationary Rossby waves. Mordvinov and Latysheva [2013] calculated the meridional component of the group velocity of Rossby waves and compared it with reanalysis data. In the β-plane approximation, the expression for the meridional component of the group velocity has the form

$$c_{gv} = 2\beta km \Big/ \left(k^2 + m^2 + l^2/gh\right)^2, \quad (1)$$

where β is the Rossby parameter; k, m are the meridional and zonal wave numbers; l is the Coriolis parameter; g is the free fall acceleration; h is the height of the uniform atmosphere (~8000 m).

The disturbance trajectories calculated using this formula for Rossby waves with zonal wave numbers m=1, 2, 3 were plotted on torsional oscillation diagrams and showed good agreement. One of the objections to this interpretation is that torsional oscillations occur equally in both the Northern and Southern hemispheres, yet in the Southern Hemisphere stationary waves have a much lower amplitude and hence should produce weaker secondary disturbances when interacting with traveling Rossby waves. The assumption that torsional oscillations can be eigenoscillations of the atmosphere remains, therefore, valid. In this case, they should have an axisymmetric component and a meridional velocity component of ~6°/day. We can assume that polar vortices are of great importance in their formation since sources of torsional oscillations are recorded in the polar region.

We have previously studied the NNM dependences on the mean flow in a simple barotropic model of differential rotation of the solar atmosphere in the tachocline region [Mordvinov et al., 2013]. The main attention in that paper was, however, paid to the rates of NNM increase, and not to their spatial structure, since the layer in which the instabilities develop has a thick convective shell masking the structure of the flows beneath it. In Earth's atmosphere, observations provide more complete information, which makes it possible to analyze not only the growth rates and periods of eigenoscillations, but also their spatial structure.

Mordvinov and Zorkaltseva [2022] have really obtained normal modes similar in structure to torsional oscillations, yet could not reproduce all properties of the oscillations. The main problem is to parameterize the mean flow. Flows in the atmosphere are constantly changing; it is, therefore, difficult to choose any specific synoptic configurations as a possible source of the oscillations we are interested in. This is especially difficult to do in the troposphere. In the stratosphere, flows have a simpler configuration, and it becomes possible to resolve such a problem. In this paper, we use the polar cyclone + anticyclone configuration, which is the most common in the lower stratosphere, in our calculations to study NNM at this level and to try to interpret torsional oscillations.

MODEL

We adopt the same mathematical flow model as in [Mordvinov et al., 2023]. The method of solving the problem was described in [Mordvinov et al., 2013]. To describe the flow, we use the barotropic equation of quasi-geostrophic potential vortex [Dikpati, Gilman, 2001; Dymnikov, Filatov, 1988]:

$$\frac{\partial\left(\Delta-L_0^{-2}\right)\psi}{\partial t}=\frac{1}{a^2}\left[\frac{\partial\psi}{\partial\mu}\frac{\partial\Delta\psi}{\partial\lambda}-\frac{\partial\psi}{\partial\lambda}\frac{\partial\Delta\psi}{\partial\mu}\right]- \\ -\frac{2\Omega}{a^2}\frac{\partial\psi}{\partial\lambda}-r\Delta\psi-K\Delta^N\left(\Delta\psi\right), \tag{2}$$

where ψ is the stream function related to the horizontal velocity vector by the relation

$\mathbf{v}=\mathbf{k}\times\nabla\psi=\left(-\mathbf{i}\frac{\partial\psi}{\partial y}, j\frac{\partial\psi}{\partial x}\right)$; λ is the longitude; $\mu=\cos\theta$; θ is the polar angle (latitude); a is the Earth radius; Ω is the Earth angular velocity; $L_0\equiv\sqrt{gh}/l\approx\sqrt{gh}/2\Omega\sin 45^\circ$ is the Rossby — Obukhov radius; r is the Rayleigh friction coefficient, assumed to be 10 days^{-1}; K is the coefficient of turbulent viscosity; N is the parameter that determines the accepted model of viscosity parameterization. For ordinary turbulent viscosity $N=1$, and the coefficient K is equal to the coefficient of effective turbulent kinematic viscosity v. Parameterizations $N>1$ correspond to hyperviscosity. We have considered two variants of hyperviscosity — $N=2$ and $N=3$. We solved the problem in spherical geometry by expanding stream function perturbations with respect to spherical functions. When approximating the fields, we used a triangular truncation.

After linearization, substitute the solution of the perturbation equation as a normal mode

$$\psi'\left(\lambda,\mu,t\right)=e^{\sigma' t}\sum_\gamma\psi_\gamma Y_\gamma\left(\mu,\lambda\right). \tag{3}$$

In this expression, σ' determines the rate of normal mode amplitude increase (or damping) (increment/decrement), and the superposition of spherical functions $Y_\gamma(\mu, \lambda)$ characterizes the spatial structure of the normal mode. Both values are complex. The substitution yields the problem of eigenvalues and eigenfunctions of the D operator:

$$D\psi'_0=\sigma'\psi'_0, \tag{4}$$

$$D_{\gamma\gamma'}=\frac{1}{k_{n'}\Omega}\left\{\sum_\gamma\psi_\gamma\int_S Y^*_{\gamma'}J\left(Y_\gamma,G'_n\right)dS\right\}- \\ -\delta_{\gamma\gamma'}\left[i\frac{2m'}{k_{n'}}+r_1\right], \tag{5}$$

where

$J\left(f,g\right)\equiv\frac{\partial f}{\partial\lambda}\frac{\partial g}{\partial\mu}-\frac{\partial f}{\partial\mu}\frac{\partial g}{\partial\lambda}$; $G'_n=\Delta\bar{\psi}+k_n\bar{\psi}$; $\sigma'=\sigma/\Omega$;

$\gamma=\left(m,n\right)=\left(m_\gamma,n_\gamma\right)$ is the wave vector; m is the order of the spherical function in the expansion (zonal wavenumber); n is the degree of spherical function $Y_\gamma\left(\mu,\lambda\right)$,

$r_1=r/\Omega+Kn^N\left(n+1\right)^N/\Omega a^4$, $k_n=n\left(n+1\right)$.

Elements of the D matrix depend on the mean flow $\bar{\psi}\left(\mu,\lambda\right)$. The number of spherical functions in the field expansion ψ' determines the size of the D matrix; and the viscosity parameterization, diagonal terms of the r_1 matrix. It is convenient to write the viscous term as $r_1=\gamma\left(\gamma+1\right)\left(r_t+g_N\gamma^N\left(\gamma+1\right)^N\right)$. In the absence of turbulent viscosity, g_0=0. For ordinary turbulent viscosity, $N=1$. For the hyperviscosities $N=2$ and $N=3$, coefficients g_1, g_2, and g_3 were calculated from the condition of equality of hyperviscosity of the ordinary turbulent viscosity for the selected harmonic. For example, if a

harmonic having a degree γ' is chosen, the equation for finding the coefficient g_N looks like $r_t = g_N \gamma'^N (\gamma'+1)^N$. Figure 1 plots the viscosity term versus the degree of spherical function for $\gamma' = 10$ (*a*) and $\gamma' = 20$ (*b*).

We use a simplified viscosity parameterization. This is primarily due to the two-dimensionality of the problem [Danilov, Gurari, 2000]. For barotropic processes having a horizontal scale far exceeding the characteristic height of the atmosphere, the very concept of viscosity becomes less defined. Along with the effects of damping of disturbances, we should take into account their intensification due to the combined effect of baroclinic waves and vortices on the barotropic component — the so-called negative viscosity. It is very difficult to calculate, and even estimate, this driving force. In some cases, in particular during blocking in the troposphere, this driving force is completely balanced out by the ordinary viscosity and the turbulent viscosity term can be ignored [Dymnikov, Filatov, 1988; Dymnikov, 2007]. In the linearized problem of eigenfunctions and eigenvalues, such complications make no sense at all and the viscosity is parameterized in the form we used. A result of the simplifications is the inability to relate the calculations to specific synoptic situations. They have to be considered only as a statistical trend. This, nonetheless, fully corresponds to the very concept of torsional oscillations, which are also statistically identified after averaging and filtering [Zorkaltseva et al., 2019].

The procedure for specifying the mean flow $\bar{\psi}(\mu, \lambda)$, for which normal modes are computed is also simplified. We chose one of the most frequent configurations as the object of research — polar cyclone + midlatitude anticyclone, approximating the stream function of each of the vortices by a simple Gaussian. In a way, this configuration can be considered as a result of averaging of winter flows in the upper troposphere — the lower stratosphere. An alternative may be to use a climatic mean flow, as is often done, but we are interested not so much in the normal modes themselves as in their dependence on the parameters of the mean flow, and hence it is much more convenient to specify the stream function in a simplified form. However, even in such a simple variant, the location of Gaussian centers, their size and amplitude may be different. All these variables affect the calculation results, which is why the problem becomes multiparametric. Since such a problem can be solved only by numerical methods, a need arises to assess the NNM dependence not only on the structure of the mean flow, but also on parameters of numerical experiments.

RESULTS OF NUMERICAL EXPERIMENTS

As we have already noted, in the winter stratosphere of the Northern Hemisphere, the main structural features are the cyclonic vortex over the pole and the anticyclonic vortex at midlatitudes [Large-scale..., 1988]. It is known that for small meridional velocity gradients, the zonally symmetric flow of the polar vortex is stable, with large-scale normal modes being the least damping. When the anticyclonic vortex strengthens and stream function gradients increase, unstable normal modes appear. Instability grows especially rapidly with increasing zonal inhomogeneity of the mean flow. Verify these preliminary conclusions numerically.

Define the stream function of the mean flow as the sum of two Gaussians $\bar{\psi} = a_1 \exp\{-k_1 p^2\} + a_2 \exp\{-k_2 p^2\}$, corresponding to the cyclonic vortex over the pole and the anticyclonic vortex over midlatitudes. Here p is the orthodromy (angular distance between the vortex center

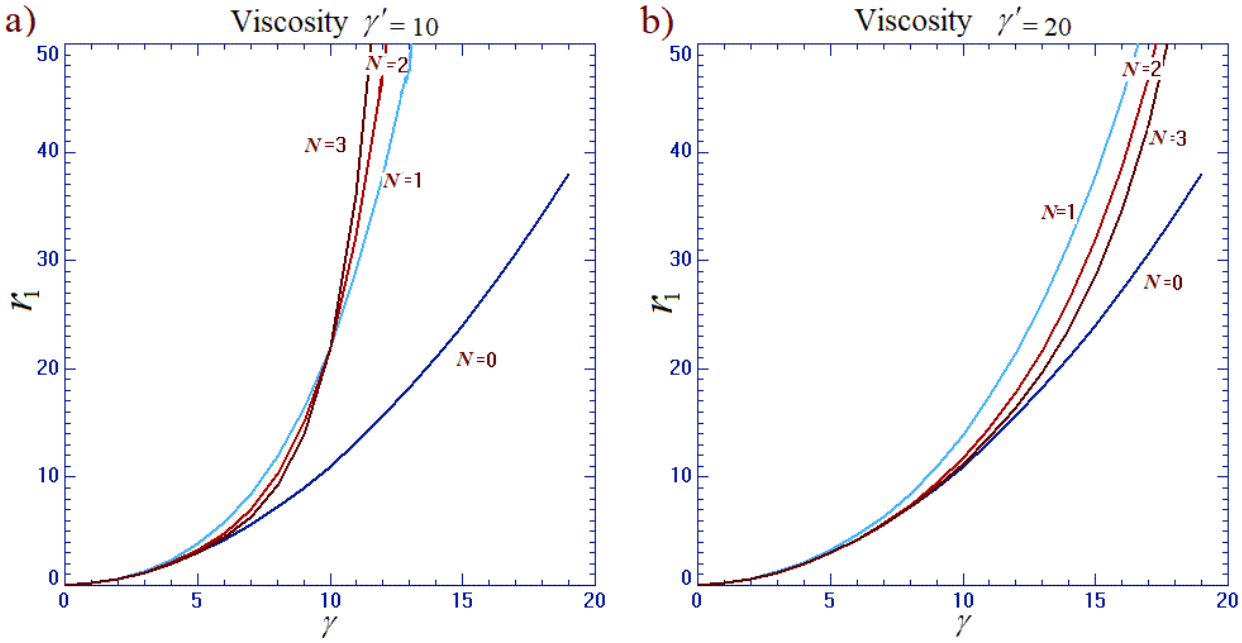

Figure 1. Viscosity dependence on the degree of spherical function for γ'=10 (*a*) and γ'=20 (*b*): blue — Rayleigh friction at $N = 0$; light blue — ordinary turbulent viscosity at $N = 1$; red and brown — hyperviscosity at $N = 2$ and $N = 3$ respectively

and an arbitrary point on the sphere); $k_{1,2}$ are the coefficients characterizing the Gaussian width, k_1=1, k_2= 1, ...6; a_1=0.5, a_2=0.5. In radians, the Gaussian width is related to the coefficient k by $\Delta = 1/\sqrt{2k}$. The anticyclone center is located at 60° N. During the numerical experiment, we change the amplitude of the anticyclonic vortex and its width. The eigenfunctions of Equation (4) are computed up to a constant factor, so NNMs do not depend on amplitudes of the vortices, but on their ratio. Accordingly, the problem can be solved not in absolute, but in relative units. Since the cyclonic vortex is centered about the pole, the ratio of vortex amplitudes determines the degree of deviation of the fluid flow from the zonally symmetric one, which is crucial for the development of instabilities. Consider how increments and spatial structure of the most unstable NNMs depend on the amplitude of the vortices and numerical experiment parameters.

1. NNM growth rate

Figure 2 plots characteristic times of increase in amplitudes of the most unstable NNMs $t = 1/\sigma'$ (day) as function of the anticyclone amplitude a_2 for different numbers of harmonics in the stream function expansion, with different viscosity parameterizations and selected harmonics $l = \gamma' = 10$ and $l = \gamma' = 20$. Plots of dark blue color correspond to the number of harmonics n_{max} in expansion, 13; blue, 15; red, 17; brown, 19.

Note immediately that for the harmonic $l = \gamma' = 20$ results of increment calculations practically coincide with the results of calculations for ordinary turbulent viscosity. For the harmonic $l = \gamma' = 10$, calculations with higher hyperviscosity orders N show a rise in the characteristic time of increase in amplitudes of the most unstable normal modes, i.e. an increase in the hyperviscosity order reduces the growth rate of instabilities. However, at the highest amplitude of the anticyclone, the amplitude increments depend only on the number of harmonics in the stream function expansion rather than on the order of hyperviscosity.

The plots corresponding to n_{max}=15 (blue) demonstrate an unusual dependence on anticyclone amplitude. With an axisymmetric cyclonic mean flow, the flow turns out to be more unstable than with the superposition of the cyclonic vortex and the low-amplitude anticyclone. With a further increase in the anticyclone amplitude, instability increases, and the characteristic time of increase in the NNM amplitude decreases. For the number of harmonics in the expansion n_{max} =17 (red) and n_{max}=19 (brown), there is no such feature on the plots, the degree of instability increases smoothly as the number of harmonics and the anticyclone amplitude increase. We cannot yet explain features of the plots for n_{max}=15.

Except for the feature at n_{max}=15, the dependences of instability increments on the anticyclonic vortex amplitude proved to be quite expected — rates of increase in the amplitude of the most unstable modes rose with increasing amplitude of anticyclonic vortex. Nonetheless, they also depend on the number of harmonics in the expansion — when n_{max} changes from 15 to 19, the characteristic time of instability development changes by 50–100 %. To a somewhat lesser extent, but within approximately the same range, the calculation results depend on parameterization of hyperviscosity. With a further increase in the number of harmonics in the expansion, these differences should probably decrease. This is evidenced by theoretical assessments of the convergence of calculations of D eigenvalues and their estimates [Dymnikov, Skiba, 1986].

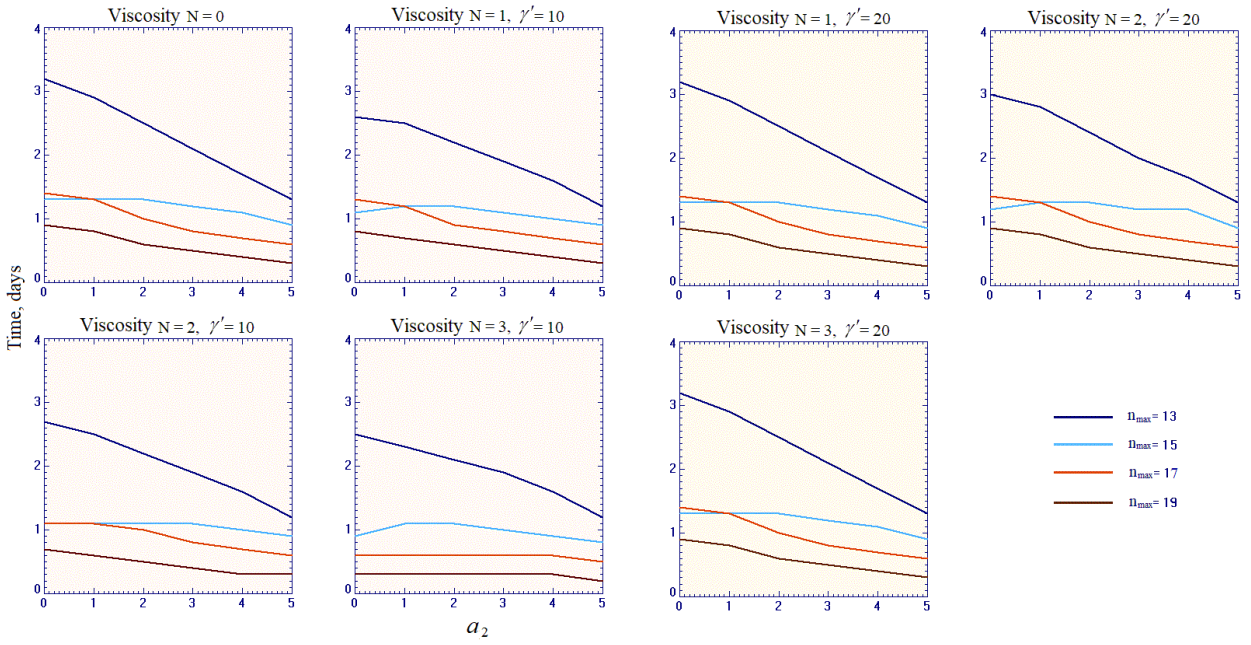

Figure 2. Characteristic times of increase in amplitude of the most unstable NNMs as function of the anticyclone amplitude for different numbers of harmonics in the expansion: dark blue — n_{max}=13, blue — n_{max}=15, red — n_{max}=17, brown — n_{max}=19

2. NNM spatial structure

A more difficult problem is to estimate changes in the NNM spatial structure depending on changes in the mean flow and numerical experiment parameters. For the analysis, we have used two representations of the NNM spatial structure — maps of NNM stream function distributions and NNM spectra in spherical function expansion. The former method is convenient for visual analysis and qualitative comparison. The latter method is less descriptive, but it allows us to quantify some characteristics of the NNM structure.

In Figure 3, *a*, *b*, columns 1, 2 illustrate distributions of the stream function of the fastest increasing NNMs at different mean flow configurations, depicted in the polar projection in columns 4. The normal mode stream function distributions are given in horizontal (columns 1) and polar (columns 2) projections. In all cases, the mean flow is a superposition of the polar cyclonic vortex and the anticyclonic vortex at midlatitudes. The anticyclonic vortex amplitude increases in the Figures from top to bottom. NNMs are plotted for 13 (*a*) and 15 (*b*) harmonics in the field expansion at ordinary turbulent viscosity. Each panel in columns 1 shows characteristic times of increase in the NNM amplitude (*T*) and the oscillation period (*T*1). In columns 3 are isolines of NNM spectra in the coordinates *n* (X-axis) and *n*+*m* (Y-axis). Axisymmetric harmonics are located on the diagonal blue line $y = x$. On the NNM spectra are plots of the energy dependence of spherical functions on the degree *n* in the expansion of NNMs in harmonics. By the spherical harmonic energy is meant the sum of squares of the real and imaginary coefficients in the expansion. It can be seen, for example, that in the spectrum of the most unstable mode with an axisymmetric mean flow and 13 harmonics, only one spherical function (axisymmetric) prevails in the expansion, for which n=5, m=0, the time of amplitude increase *e* times is 2.64 days, and the oscillation period is 7916 days, i.e. this NNM is stationary.

Figure 4 exhibits the most unstable NNMs for the same configurations of the mean flow as in Figure 3, but for 17 (*a*) and 19 (*b*) harmonics in the stream function field expansion.

With the number of harmonics in the expansions n_{max}=13 (*a*) and n_{max}=15 (*b*), modes with the axisymmetric structure are seen to prevail (7 of 12 cases). They have a different number of sign changes along the meridian, different oscillation periods, and different increments. At n_{max}=17 and n_{max}=19, the axisymmetric modes are at least not the most unstable. In 8 of 24 cases, the structure of the most unstable modes was almost unchanged with a variation in the anticyclone amplitude (6 cases at n_{max}=17 and n_{max}=19, and 2 cases at n_{max}=15), but in other cases the changes in the structure of unstable modes were large. For clarity, in Figure 5 we have plotted composite spectra of the most unstable modes in the coordinates *n*, $n+m$ at different viscosity parameterizations (from top to bottom: N=0, 1, 2, 3), the number of spherical harmonics in the expansion (from left to right: n_{max}=13, 15, 17, and 19), and anticyclonic vortex amplitudes (a_2=0... 5) The dark blue color corresponds to zero anticyclone amplitude (zonally symmetric flow), blue — 1, light blue — 2, turquoise — 3, beige — 4, orange — 5. At N=0, there is no turbulent viscosity; at N=1, the turbulent viscosity is ordinary; N=2, 3 correspond to hyperviscosities of degrees 2 and 3.

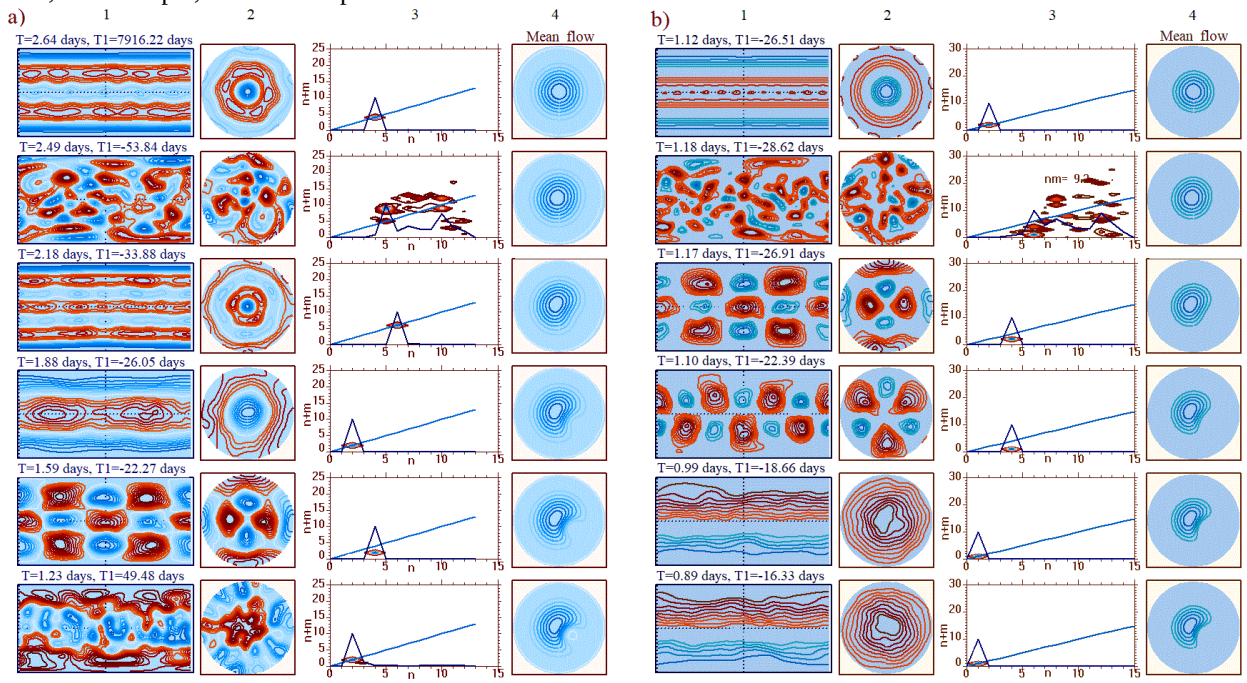

Figure 3. The most unstable NNMs at different configurations of the mean flow for 13 (*a*) and 15 (*b*) harmonics in the field expansion at ordinary turbulent viscosity. In Figures *a* and *b* from left to right are NNM stream functions in horizontal and polar projections, NNM spectra in coordinates *n* (X-axis) and *n*+*m* (Y-axis), and distributions of the stream function of the mean flow in the polar projection in relative units

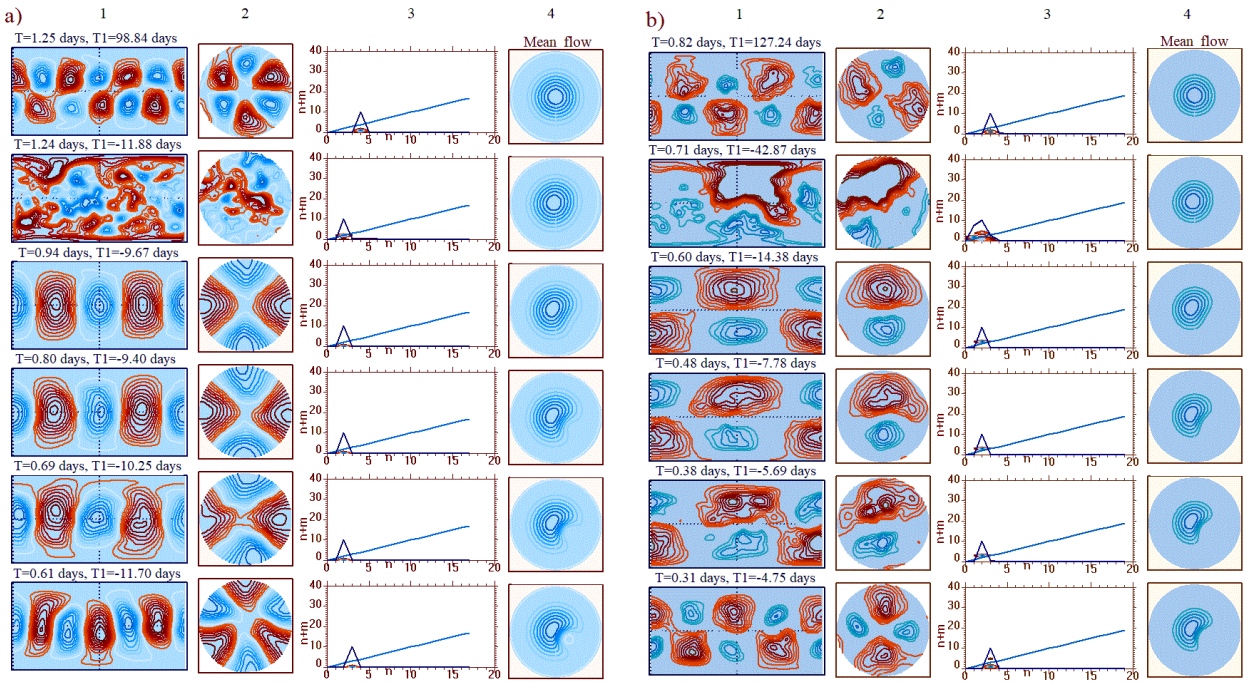

Figure 4. The same as in Figure 3, but for 17 (*a*) and 19 (*b*) harmonics in the field expansion

The results of calculations of the spectra show that the structure of the most unstable NNMs depends heavily on the number of harmonics in the expansion (see Figures 3, 4, and 5). The dependence of the spectra on the degree of hyperviscosity is probably somewhat smaller.

Spectral representation of the NNM structure in Figure 5 cannot provide information on regularities of the appearance of NNM with a particular spatial structure, especially in cases where the NNM structure is complex with a large number of harmonics in the expansion. Figure 6 plots the average degree of spherical functions in the expansion for $l = \gamma' = 10.$ versus the anticyclone amplitude a_2. Panels show calculations with viscosity parameterizations N=0, 1, 2, 3. In all cases, we took into account Rayleigh friction with a characteristic damping time of 10 days.

With the exception of the calculation results for hyperviscosity $N = 3$, the plots of the dependences of the average degree of spherical functions behave in the same way at the number of harmonics in the expansion n_{max}=17 (red) and n_{max}=19 (brown). With increasing anticyclone amplitude, the average degree of spherical functions first decreases and then increases, i.e. at first the NNM structure has a larger scale, and then higher harmonics appear again in the expansion. The behavior of the plots at n_{max}=13 (blue) and n_{max}=15 (blue) is more complex.

Note that we have identified only tendencies for the NNM structure to change depending on various factors. Unlike the NNM increments demonstrating pronounced stable dependences, the NNM spectra change more chaotically when problem parameters change, and it is impossible to predict which structure unstable NNM will have in one case or another at any given mean flow. This significantly deteriorates the applicability of the NNM method to prediction of the structure of developing flows. Apparently, without taking into account the nonlinearity of the interaction processes, it will be very difficult to identify the structure of flows during the development of instability. This conclusion also applies to the interpretation of observable oscillations, including torsional oscillations. Axisymmetric fastest-growing modes appear quite often, but they differ greatly in their meridional structure, oscillation periods, and increments. Finally, the problem of meridional propagation of oscillations remains unresolved. The effect of meridional motions can be seen at high latitudes when analyzing real and imaginary components of axisymmetric NNMs, yet it is not global in nature and we cannot confirm it with quantitative calculations. In general, the problem of interpreting torsional oscillations remains unsolved.

CONCLUSION

We have numerically computed NNMs in the barotropic quasi-geostrophic model of the flow caused by the superposition of cyclonic and anticyclonic vortices. This flow structure is often found in the circulation of the winter atmosphere in the upper troposphere or the lower stratosphere. Depending on amplitude, structure, and location of the vortices, the mean flow can be either stable or unstable. To study the initial stage of instability development, the normal mode method is often used which allows us to estimate thresholds of instability occurrence in a linear approximation depending on the mean flow structure. The normal mode method can be employed to interpret the oscillations observed in the atmosphere. Problems of both types are solved numerically, which is why calculated NNMs depend not only on the mean flow structure, but also on numerical experiment parameters. In our case, the experiment parameters

were the number of harmonics, applied to the field expansion of stream function perturbations, and viscosity parameterizations. Firstly, the NNM dependences on the mean flow and, secondly, the dependences on experiment parameters were estimated.

The behavior of increments of the fastest growing NNMs depending on external conditions proved to be simpler than NNM structures. Flow instability always increased with increasing anticyclone amplitude, of course, to varying degrees with different viscosity parameterizations and the number of spherical harmonics in the field expansion of stream function perturbations. The situation with the NNM spatial structure turned out to be more difficult. Even relatively small changes in the experiment parameters and the mean flow (anticyclone amplitude) significantly changed the structure of the most unstable NNMs. On average, with an increase in the anticyclone amplitude and the number of harmonics in the expansion, the structure of unstable modes became larger-scale, spherical functions of degrees n=1, 2 prevailed in it, yet this was not always the case. The viscosity parameterization had a less strong effect on the NNM structure.

Axisymmetric oscillations appeared quite often among the fastest growing NNMs, but they differed greatly in their meridional structure, periods, and increments. Furthermore, they did not ensure meridional propagation of disturbances, which is typical of torsional oscillations. In this regard, the numerical experiments have not given any convincing evidence in favor of the hypothesis of torsional oscillations as eigenoscillations of the atmosphere for the mean flow caused by the superposition of polar cyclone + anticyclone flows.

The work was financially supported by the Ministry of Science and Higher Education of the Russian Federation (Grant No. 075-GZ/Ts3569/278).

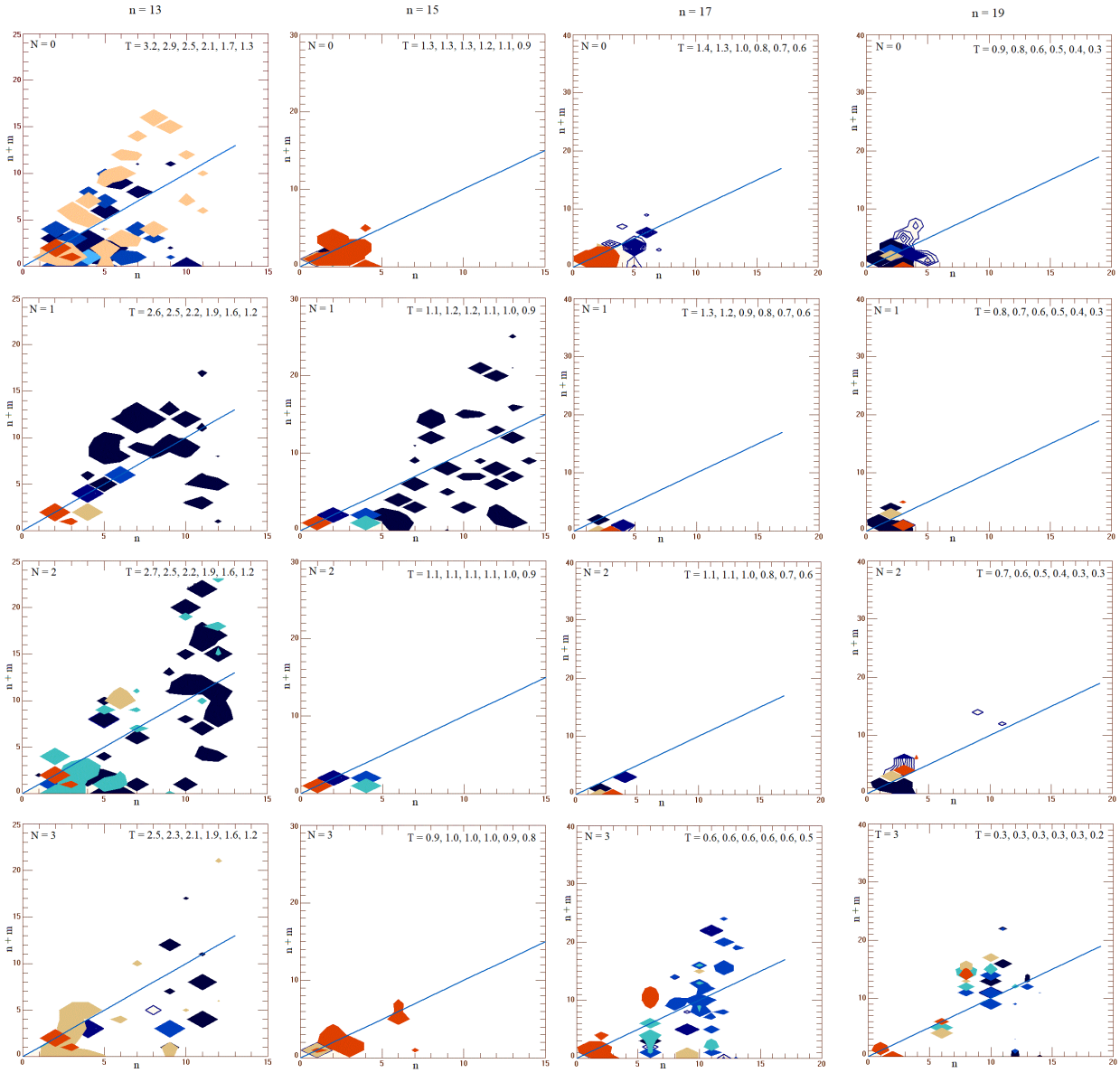

Figure 5. Composite spectra of the most unstable NNMs with viscosity parameterizations N=0, 1, 2, 3 (from top to bottom), the number of spherical harmonics in the expansion n_{max}=13, 15, 17, 19 (from left to right), and different anticyclonic vortex amplitudes (highlighted in color) $l = \gamma' = 10$. In each panel are characteristic times T of increase in amplitudes of the most unstable NNMs

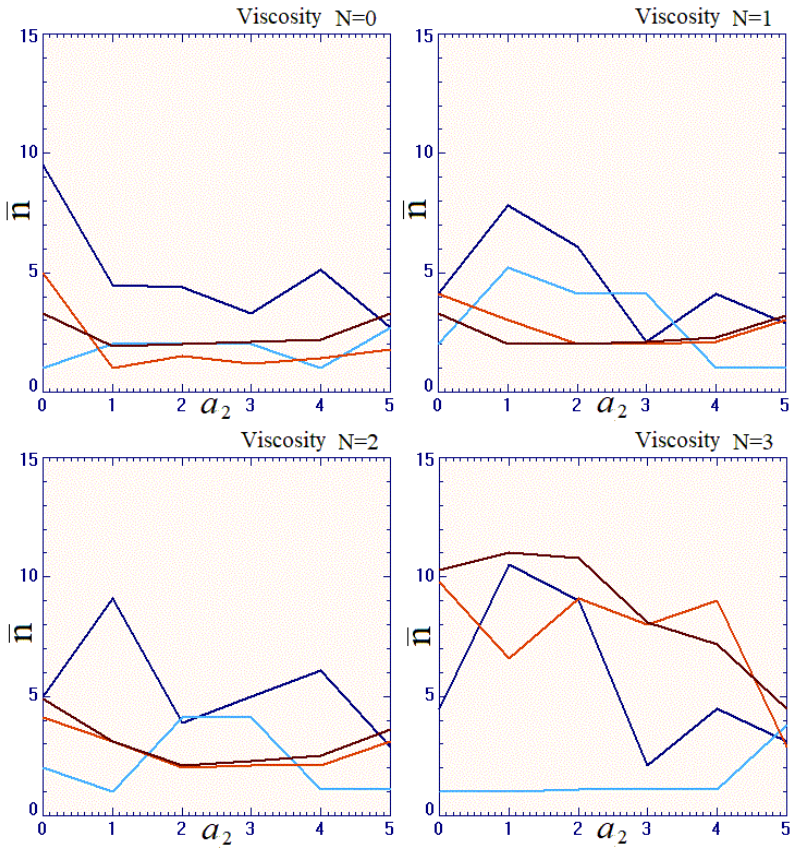

Figure 6. Average degree of spherical functions in the NNM expansion versus the anticyclone amplitude a_2 for different numbers of harmonics in the expansion: dark blue — n_{max}=13, blue — n_{max}=15, red — n_{max}=17, brown — n_{max}=19; γ'=10

REFERENCES

Blackmon M.L., Lee Y., Wallace J.M. Horizontal structure of 500 mb height fluctuations with long, intermediate and short time scales. *J. Atmos. Sci*. 1984a, vol. 41, pp. 961–980. DOI: 10.1175/1520-0469(1984)041<0961:HSOMHF>2.0.CO;2.

Blackmon M.L., Lee Y., Wallace J.M., Hsu H. Time variation of 500 mb height fluctuations with long, intermediate and short time scales as deduced from lag-correlation statistics. *J. Atmos. Sci*. 1984b, vol. 41, iss. 6, pp. 981–991. DOI: 10.1175/ 1520-0469(1984)041<0981:TVOMHF>2.0.CO;2.

Branstator G. A striking example of the atmosphere's leading travelling pattern. *J. Atmos. Sci*. 1987, vol. 44, pp. 2310–2323.

Branstator G., Held I. Westward propagating normal modes in the presence of stationary background waves. *J. Atmos. Sci*. 1995, vol. 52, pp. 247–262.

Danilov S.D., Gurarie D. Quasi-two-dimensional turbulence. *Physics – Uspekhi*. 2000, vol. 170, no. 9, pp. 863–900. DOI: 10.1070/PU2000v043n09ABEH000782.

Dikii L.A. *Theory of Vibrations of the Earth's Atmosphere*. Leningrad, Gidrometeoizdat Publ., 1969, 194 p. (In Russian).

Dymnikov V.P., Skiba Yu.N. Barotropic instability of zonally symmetric atmospheric flows. *Calculation Processes and Systems*. Moscow, Nauka Publ., 1986, iss. 4, pp. 63–104. (In Russian).

Dymnikov V.P., Filatov A.N. *Stability of Large-Scale Atmospheric Processes*. Moscow, 1988, 140 p. (In Russian).

Dymnikov V.P. *Stability and Predictability of Large-Scale Atmospheric Processes*. Moscow, IVM RAN Publ., 2007. 283 p. (In Russian).

Dikpati M., Gilman P.A. Analysis of hydrodynamic stability of solar tachocline latitudinal differential rotation using a shallow water model. *Astrophys. J. Papers*. 2001, vol. 551, no. 1, pp. 536–564. DOI: 10.1086/320080.

Kasahara A. Effect of zonal flows on the free oscillations of a barotropic atmosphere. *J. Atmos. Sci*. 1980, vol. 37, iss. 5, pp. 917–929. DOI: 10.1175/1520-0469(1980)037<0917:EOZFOT>2.0.CO;2.

Koval A.V., Gavrilov N.M,. Pogoreltsev A.I, Shevchuk N.O. Influence of solar activity on penetration of traveling planetary-scale waves from the troposphere into the thermosphere. *J. Geophys. Res.: Space Phys*. 2018, vol. 123, no. 8. P. 6888–6903. DOI: 10.1029/2018JA025680,08.2018.

Large-Scale Dynamic Processes in the Atmosphere. Moscow, Mir Publ., 1988, 430 p. (In Russian).

Longuet-Higgins M.S. Planetary waves on a rotating sphere. *Proc. Royal Soc., Series A*. 1964, vol. 279, iss. 1379, pp. 446–473.

Longuet-Higgins M.S. The eigenfunctions of Laplace's tidal equation over a sphere. *Math. and Phys. Sci*. London, 1968, vol. 262, pp. 511–607. DOI: 10.1098/RSTA.1968.0003.

Madden R.A. Large-scale free Rossby waves in the atmosphere – an update. *Tellus A: Dynamic Meteorology and Oceanography*. 2007, vol. 59, pp. 571–590. DOI: 10.1111/j.1600-0870.2007.00257.x.

Mordvinov V.I., Latysheva I.V. *Theory of General Atmospheric Circulation, Variability of Large-Scale Processes*. Irkutsk, ISU Publ., 2013, 197 p. (In Russian).

Mordvinov V.I., Zorkaltseva O.S. Normal mode as a cause of large-scale variations in the troposphere and stratosphere. *Izvestiya, Atmos. and Ocean. Phys.* 2022, vol. 58, no. 2, pp. 140–149. DOI: 10.1134/S0001433822020098.

Mordvinov V., Devyatova E., Tomozov V. Hydrodynamic instabilities in the tachocline due to layer thickness variations and mean flow inhomogeneities. *Solnechno-zemnaya fisika* [Solar-Terr. Phys.]. 2013, iss. 23, pp. 3–12. (In Russian).

Mordvinov V.I., Devyatova E.V., Tomozov V.M. Influence of the magnetic field and the mean flow configuration on

spatial structure and growth rate of normal modes. *Solar-Terr. Phys.* 2023, vol. 9, iss. 4, pp. 123–135. DOI: 10.12737/stp-94202315.

Pogoreltsev A.I., Kanukhina A.Yu., Suvorova E.V., Savenkova E. Variability of planetary waves as a signature of possible climatic changes. *J. Atmos. Solar-Terr. Phys*. 2009, vol. 71, iss. 14-15, pp. 1529–1539. DOI: 10.1016/J.JASTP.2009.05.01

Simmons A.J., Wallace J.M., Branstator G.W. Barotropic wave propagation and instability, and atmospheric teleconnection patterns. *J. Atmos. Sci*. 1983, vol. 40, no. 6, pp. 1363–1392.

Yaglom M.A. Dynamics of large-scale processes in the barotropic atmosphere. *Izvestiya AN SSSR. Seriya geofizicheskaya* [Proc. Academy of Science of USSR. Ser. Geophys.]. 1953, no. 4, pp. 346–369. (In Russian).

Zorkaltseva O.S., Mordvinov V.I., Devyatova E.V., Dombrovskaya N.S. Method for calculating torsional oscillations in Earth's atmosphere from NCEP/NCAR, MERRA-2, ECMWF ERA-40, and ERA-INTERIM. Solar-Terr. Phys. 2019, vol. 5, iss. 1, pp. 69–76. DOI: 10.12737/stp-501201910.

Original Russian version: Mordvinov V.I., Devyatova E.V., Tomozov V.M., published in Solnechno-zemnaya fizika. 2024. Vol. 10. No. 4. P. 22–30. DOI: 10.12737/szf-104202403.

How to cite this article

Mordvinov V.I., Devyatova E.V., Tomozov V.M. Dependence of normal modes of the barotropic vortex equation on the mean flow structure and numerical simulation parameters. *Solar-Terrestrial Physics*. 2024. Vol. 10. Iss. 4. P. 19–27. DOI: 10.12737/stp-104202403.